RSC Advances

ROYAL SOCIETY OF CHEMISTRY

www.rsc.org/advances

Journal Name

RSCPublishing

ARTICLE

The Effects of the Increasing Number of the Same Chromophore on Photosensitization of Water-Soluble Cyclen-based Europium Complexes with Potentials for Biological Applications

Cite this: DOI: 10.1039/x0xx00000x

Received 00th January 2014,
Accepted 00th January 2014

DOI: 10.1039/x0xx00000x

www.rsc.org/

Zhenhao Liang,[a] Chi-Fai Chan,[c] Yurong Liu,[a] Wing-Tak Wong,*[,b] Chi-Sing Lee,*[,a] Ga-Lai Law,*[,b] and Ka-Leung Wong*[,c]

Five water-soluble cyclen-based europium complexes incorporated with the pendant chelating chromophore, 2-methyl-4-(2-(4-propoxyphenyl)ethynyl)pyridine (**L**), as the antenna in different ratio had been synthesized along with full structural characterizations, photophysical measurements and in vitro biological studies. The antenna-to-metal ratios are respectively 4 (Eu-4**L**), 3 (Eu-3**L**), 2 (1,4-disubstituted Eu-o-2**L** and 1,7-disubstituted Eu-p-2**L**) and 1 (Eu-1**L**). It had been found that the definitive distinction between Eu-o-2**L** and Eu-p-2**L** can be interpreted from the emission spectra of Eu^{3+} at room and low temperature; With all together the results from subcellular stability testing (via titrations), in vitro imaging, cytotoxicity assays and cellular uptake profile, Eu-4**L** with an overall +3 charge had been demonstrated subcellular localization towards lysosomes and potentials as a selective time-resolved bio-labelling probe.

Introduction

Lanthanide series, otherwise known as rare earth elements, are the first-row f-block metals well-known for their unique photophysical and chemical properties.[1] Painstaking considerations of selecting the chelating systems for long-lived, hypersensitive, and sharply luminescent lanthanide materials encompass in general (i) energy transfer efficiency, (ii) quantum yield efficiency, and (iii) the nature of the metal complexation.[2-3] Literature-wise, most common ligands in use are nitrogen-based macrocyclic ligands, such as cyclen, triaozane, triazine, and porphyrin that serve as the antenna for transferring energy to the lanthanide ions and thus overcome the Laporte forbidden lanthanide 4fN-4fN transition.[4-6] When it comes to bioimaging, it is very true that all the above lanthanide complexes formed have been advancing the field (as time-resolved imaging agents) significantly; however, along with the development of lanthanide bioprobes, systematic studies of them in aqueous and in vitro simultaneously are still very rare. Most of the literature studies, in fact, focus on their skeleton structure-photophysical properties relationship only with the use of the same antenna.[7-8] Data about if there is any effect due to the different number of or the different spatial arrangement of the antenna are therefore still lacking. In 2010, Walton et al. reported a series of europium (III) complexes bearing one to four coordinated azaxanthone groups.[9] Recently, we have also reported the control of the number of terdentate *N*-donor pyridine ligands to improve the antenna effect of lanthanide complexes; their quantum efficiencies and kinetic data had been compared between trivalent lanthanide cations and the number of *N*-ligands under different experimental conditions.[10] That said, to develop lanthanide complexes for practical biological applications, full characterizations of them should be done ambiguously in aqueous solution, and this is particularly difficult. The ^{1}H NMR or HRMS (high resolution mass spectra), more challengingly, do not provide a definitive distinction for the isomerism between the two antennae in cyclen-based europium system. Thanks to the room and low-temperature Eu^{3+} luminescence, we can in this work give a clear identification for them. Herein, we reported the synthesis of five new europium complexes based on the cyclen skeleton with different numbers of the antenna, 2-methyl-4-(2-(4-propoxyphenyl)ethynyl)pyridine (**L**), attached (Fig. 1). The room- and low-temperature photophysical

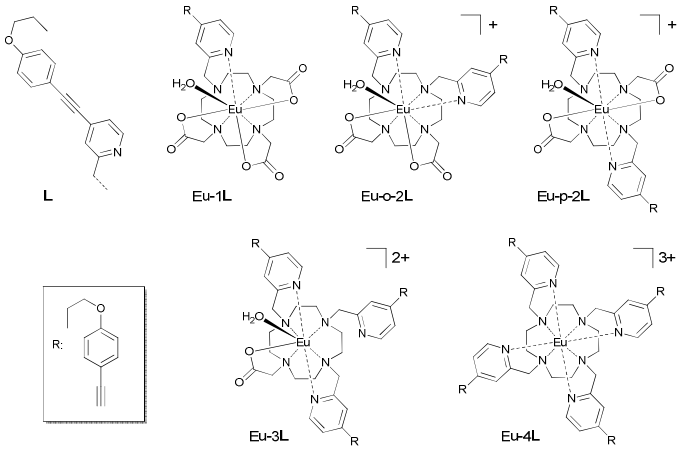

Fig. 1 The molecular structures of the ligand **L**: 2-methyl-4-(2-(4-propoxyphenyl)ethy-nyl)pyridine and their cyclen-based europium complexes.

measurements had been employed in solution to gain insights from the coordination modes against hypersensitive europium that can provide essential information for the further development of lanthanide complexes as luminescent bioprobes.

Results and discussion

Synthesis of cyclen-based europium complexes with various numbers of the same antenna

Europium complexes Eu-1**L**, Eu-o-2**L** and Eu-p-2**L** were prepared in a similar synthetic strategy. As shown in Scheme 1, alcohol **1** was converted to bromide **2** in 72% yield via the mesylation/bromination protocol.[10] Alkylation of bromide **2** with cyclenderivatives[11] **3**, **4** and **5** gave ligands 1**L**, o-2**L** and p-2**L** respectively in 62-75% yields. After acid hydrolysis of the *t*-butyl esters with TFA, the Eu complexes were prepared by treatment of $EuCl_3{\cdot}(H_2O)_6$ at neural pH. Recrystallization of the crude Eu complexes with diethyl ether afforded Eu-1**L** in 75% yield, Eu-o-2**L** in 73% yield and Eu-p-2**L** in 73% yield. Synthesis of Eu complexes Eu-3**L** and Eu-4**L** were showed in Scheme 2. Direct alkylation of cyclen with 3.6 equivalents of bromide **2** generated the tri-substituted cyclen derivative (**6**) and ligand 4**L** in 30% and 45% yield respectively. Eu complex Eu-4**L** was prepared by the treatment of ligand 4**L** with europium chloride salt in acetonitrile. Ligand 3**L** was obtained via alklyation of **6** with *t*-butyl 2-bromoacetate. Deprotection of the *t*-butyl ester group followed by complexation with europium chloride salt afforded Eu-3**L** in 63% yield. All the ligands (1**L**, o-2**L**, p-2**L**, 3**L** and 4**L**) were characterized unambiguously by ^1H, ^{13}C NMR and HRMS and the corresponding Eu complexes were characterized unambiguously by HRMS and HPLC.

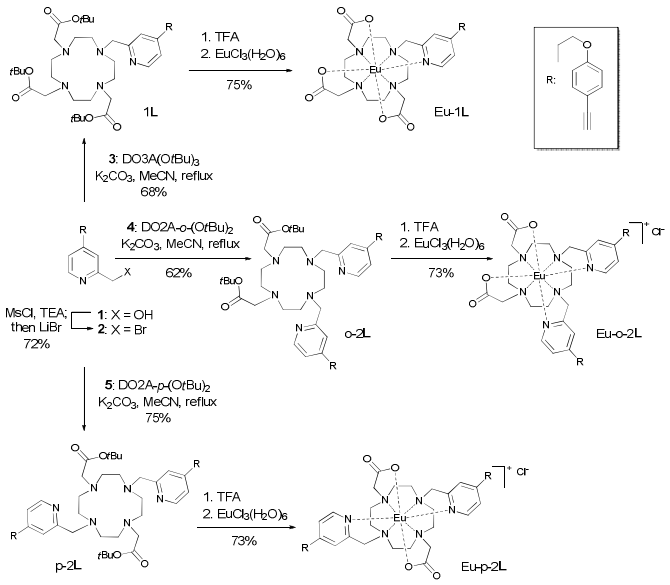

Scheme 1 Synthesis of Eu-1**L**, Eu-o-2**L** and Eu-p-2**L**

The reverse-phase HPLC analysis of these five europium complexes was carried out at room temperature by using an Agilent ZORBAX SB-C18 Stable Bond Analytical 4.6 X 150 mm 5-micron column. The mobile phase is 0.1% formic acid in milli-Q (mQ) water and 0.1% formic acid in MeCN solvent system, and the flow rate is 1.0 mL/min. Solvent gradient program is listed in the Table S1 (see supporting information). Under the given experimental condition above, the retention times of the five europium complexes are: Eu-1**L** in 10.48 min, Eu-p-2**L** in 10.93 min, Eu-o-2**L** in 11.04 min, Eu-3**L** in 10.62 min and Eu-4**L** in 11.33 min.

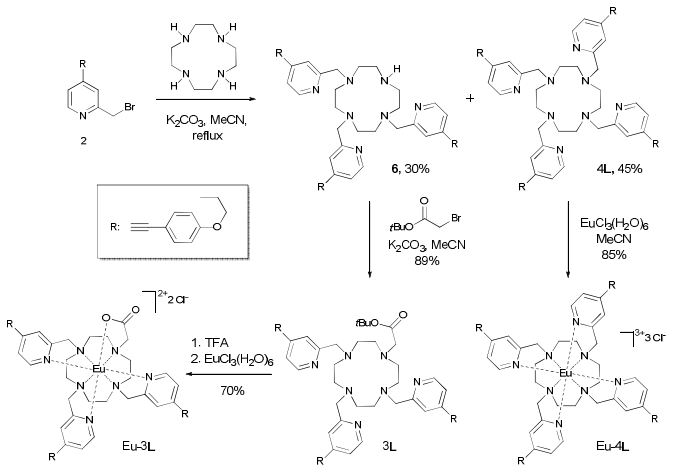

Scheme 2 Synthesis of Eu-3**L** and Eu-4**L**

The ligands and the europium complexes were analyzed by ^1H NMR spectroscopy. In CD_3OD at room temperature, the ^1H NMR spectrum of ligand 4**L** in CD_3OD displays broad signals for both the azamacrocyclic protons and the pridinyl protons. On the other hand, the Eu-4**L** exhibits a well-resolved ^1H NMR spectrum, ranging over 35 ppm due to the paramagnetism of the europium ion (Fig. 2). Only one set of the paramagnetically shifted resonance signals was observed, which is in agreement with local C_4 symmetry of Eu-4**L**. The pendant arms (ranging from 2.5 to 3.6 ppm) at room temperature became well-resolved upon complexation due to the rigidification of the macrocyclic ligand. As a result, the azamacrocyclic protons and pyridinyl protons of the pendant arms, which are in the closer vicinity of the metal, are strongly field-shifted (at 15.0 ppm, -0.3 ppm, -6.5 ppm, -7.8 ppm, -8.2 ppm, -13.3 ppm, -14.0 ppm and -16.5 ppm) and show large *J* coupling constants. In addition, directly coordinating to the europium ion via the available donor nitrogen in the π system results in high-field shift of the protons in the pyridine

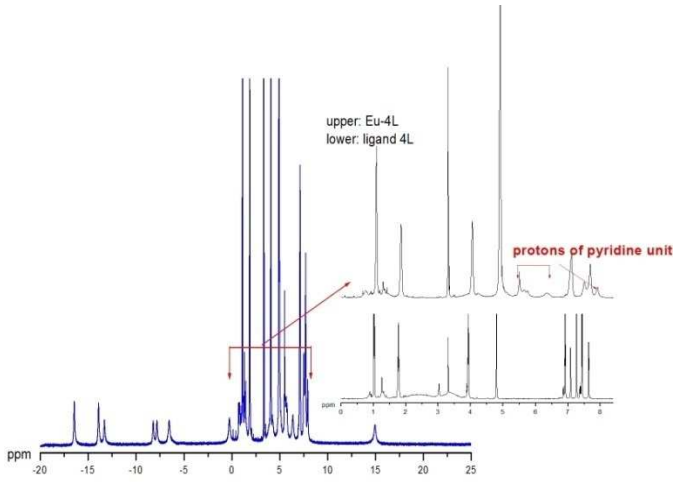

Fig. 2 ^1H NMR (500 MHz, 298 K) spectrum of Eu-4**L** in CD_3OD.

moiety (in the 5.5 - 6.4 ppm range). The mono-cationic complex, Eu-p-2**L**, gives rise to two sets of paramagnetically shifted resonance signals in CD_3OD at room temperature (Fig. 3), which is consistent with the presence of two diastereoisomeric species with C_2 symmetry, and the shifts showed a similar correspondence with those observed for Eu-4**L**. The CH_2 protons α to the carboxylates in Eu-p-2**L** occupy the positions at 24.5 ppm, 23.60 ppm, -21.1 ppm and -25.7 ppm. For the complexes Eu-1**L**, Eu-o-2**L** and Eu-3**L**, the ^{1}H NMR spectral width corresponds well with that of Eu-p-2**L**. But the spectrum is rather broad and not well-resolved, due to the presence of chemical exchange among various isomers (see Supporting information).[12]

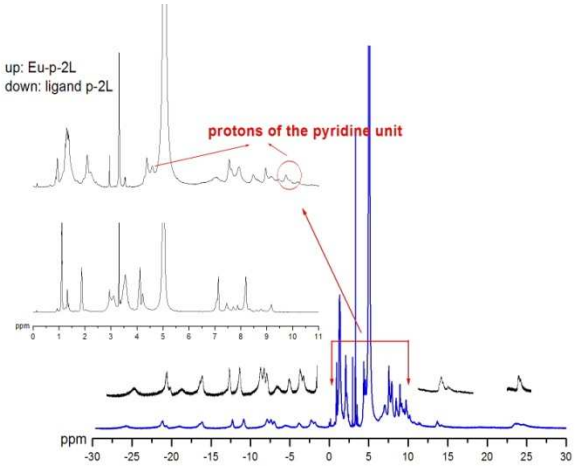

Fig. 3 ^{1}H NMR (500 MHz, 298 K) spectrum of Eu-p-2**L** in CD_3OD.

Photophysical Properties of the five water-soluble europium complexes

The choice of ligand and number of ligands for complexation plays a key role in constructing efficient luminescent lanthanide complexes; especially for biological applications (i.e. overall charge for cellular uptake, solubility for biological medium). This is very interesting and important area to be explored, but there are very limited studies to have all five complexes soluble in water with the change of number and position of ligand in complexes. Therefore, it gives the opportunity to run comprehensive studies to evaluate the effect on increasing the number of same antenna on the cyclen based skeleton as well as spatial arrangement in aqueous solution and even in vitro. The electronic absorption, emission and excitation spectra were recorded for the five Eu^{3+} complexes at 298 K (Eu-o-2**L** and Eu-p-2**L** are also recorded at 77 K) in the aqueous solution state. We are aimed to understand the effect on triplet state of the increased ligand(s) number in these five complexes. The motif Gd complexes of Eu-1**L**, Eu-o-2**L**, Eu-p-2**L**, Eu-3**L** and Eu-4**L** had been synthesized and their phosphoresence bands at 77 K monitored.

Absorption and excitation spectra of the five water-soluble europium complexes

The UV absorption spectra of five complexes are shown in Fig. 4 and their absorption coefficients are listed in Table 2. The absorption band(s) of these complexes are originated from the antenna. All five complexes have showed 481 cm^{-1} red shifted after europium complexation. Eu-4**L** with four antennae has, as expected, demonstrated the molar extinction coefficient at 325 nm (Eu-1**L**: 4318.6 $M^{-1}cm^{-1}$; Eu-o-2**L**: 11413.5 $M^{-1}cm^{-1}$; Eu-p-2**L**: 1063.37 $M^{-1}cm^{-1}$; Eu-3**L**: 14824.3 $M^{-1}cm^{-1}$; Eu-4**L**: 20454.6 $M^{-1}cm^{-1}$). For Eu-o-2**L** and Eu-p-2**L**, two antennas are conjugated at the 1,4 and 1,7 position respectively. Eu-o-2**L** has showed a slightly larger antenna coefficient (energy transfer coefficient) as the two antenna in 1,4 position are closer. In addition, the 325 nm absorption band in Eu-3**L** and Eu-4**L** are very strong as there of the antenna. The excitation spectra of all five complexes under the same experimental conditions (concentration = 1 μM in water) were also recorded and have showed the board excitation band at 340 nm, similar to the absorption band.

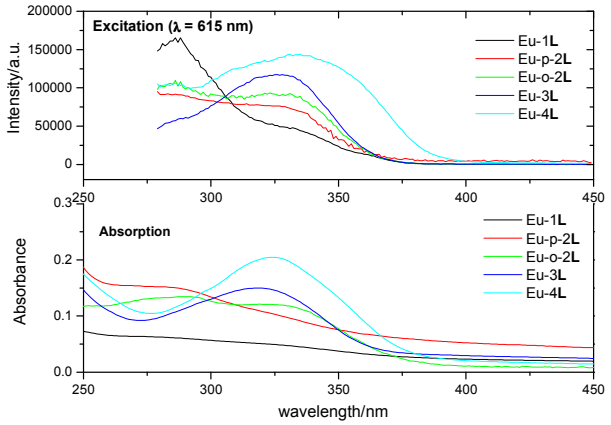

Fig. 4 Excitation (upper) and UV absorption (lower) spectra of the five complexes in aqueous solution (10 μM in water).

Room temperature emission spectra of the five water-soluble europium complexes (Eu-1L; Eu-o-2L; Eu-p-2L; Eu-3L and Eu-4L)

There are limited examples for the comparison of photophysical properties of cyclen-based lanthanide complexes with various numbers of the same antenna in the same solution

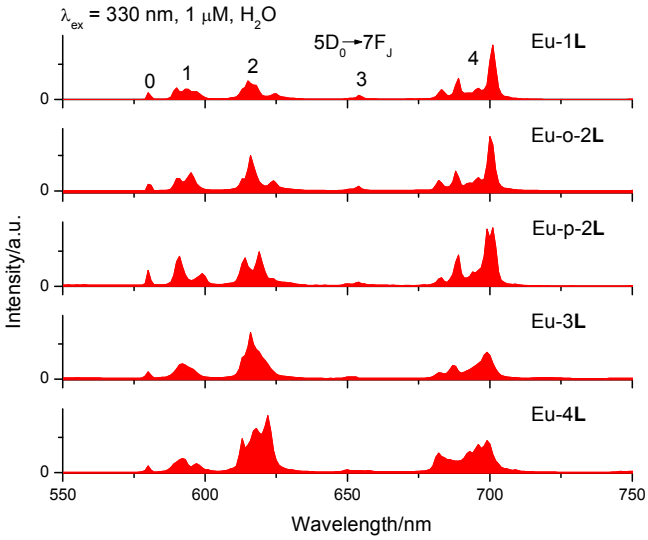

Fig. 5 Emission spectra of five europium complexes of Eu-1**L**, Eu-p-2**L**, Eu-o-2**L**, Eu-3**L** and Eu-4**L** in aqueous solution, 1 μM (λ_{ex} = 330 nm).

Table 1 The ratios of $^5D_0 \rightarrow {}^7F_J$ (J = 0-4) emission bands of five water-soluble europium complexes (Eu-1**L**; Eu-o-2**L**; Eu-p-2**L**; Eu-3**L** and Eu-4**L**) in Fig. 5.

$^5D_0 \rightarrow$	$^7F_0$	$^7F_1$	$^7F_2$	$^7F_3$	$^7F_4$
Eu-1**L**	0.64	1	1.56	0.40	4.51
Eu-o-2**L**	0.39	1	1.89	0.29	2.92
Eu-p-2**L**	0.54	1	1.15	1.70	1.73
Eu-3**L**	0.51	1	2.92	0.16	1.70
Eu-4**L**	0.53	1	3.85	0.12	2.15

Table 2 The photophysical and kinetic data of five water soluble europium complexes (Eu-1**L**; Eu-o-2**L**; Eu-p-2**L**; Eu-3**L** and Eu-4**L**) in Fig. 5.[a]

	Eu-1**L**	Eu-o-2**L**	Eu-p-2**L**	Eu-3**L**	Eu-4**L**
$\varepsilon_{325nm}/M^{-1}cm^{-1}$	4318.6	11413.5	10633.7	14824.3	20454.6
τ_{H2O}/ms	0.33	0.72	0.52	0.36	0.57
τ_{D2O}/ms	1.03	1.48	1.22	1.1	0.58
q[b]	1.0	0.56	1.0	1.1	0
τ_{rad}^{-1}	0.429	0.334	0.45	0.33	0.406
Q_{Eu}^{L} [c]	1.6	4.5	3.3	13.3	14.5
η_{sen}	0.073	0.082	0.47	0.98	0.69
pKa	5.1	4.9	4.6	5.4	5.3

[a] ε : the molar extinction coefficient, τ_{H2O} : luminescence lifetimes in H_2O, τ_{D2O} : luminescence lifetimes in D_2O (for Europium, the lifetime of the excited state $^5D_0$ to $^7F_2$), q : the number of coordinated water molecules, τ_{rad} : the radiative (or natural) lifetimes of the $^5D_0$ state, Q_{Eu}^{L} : the overall quantum yield upon ligand excitation, η_{sen} : the sensitization efficiencies of the Eu^{3+} $^5D_0$ luminescent state.[13,14] [b] Values of the number coordinated water molecules, q, (±20%), were determined according to ref.[15,16] The non-integral q-value of Eu-o-2**L** could due to (i) the equilibrium distribution; (ii) the hydration impact of a relatively distant, loosely bound water molecule in the second-coordination sphere that exchanges in an one-or-nothing manner.[15,16] [c] The quantum yield was measured by integrated sphere in aqueous solution.

medium, especially available in aqueous solution. The emission spectra of the five europium complexes were measured with the excitation at 330 nm in aqueous solution and shown in Fig. 5 which had been arbitrarily scaled. All the $^5D_0 \rightarrow {}^7F_J$ transitions (J = 0 to 4) of europium in five complexes are detected and marked in Fig. 5. The increases in the $^7F_1$ (magnetic dipole) to $^7F_2$ (electric dipole) ratio are listed in the Table 1, indicating the change from unsymmetrical Eu-1**L** to symmetrical Eu-4**L**.The $^5D_0$ to $^7F_0$ transition at 580 nm diminished in relative intensity over the series and is weakest for Eu-4**L** that is eight coordinated in solution and in C_4 symmetry. This is largely correlated to the ^{1}H NMR spectrum in Fig. 2; furthermore, this has been supported by the q-value of Eu-4**L** which is determined to be zero (Table 2). The result is overall correlated to the findings by Walton et al. as well in C_4 symmetric cyclen-based europium with three identical antennae and the ration of $^5D_0$ to $^7F_1$ to $^7F_2$ in Eu-1**L**, Eu-p-2**L**, and Eu-3**L** are almost constant. In Walton's studies, they had not reported the two antennae at the adjacent position in cyclen skeleton. Our measurements had found that the $^5D_0$ to $^7F_1$ to $^7F_2$ in Eu-o-2**L** are similar to the other three, thereby completing the missing data in the literature. The emission lifetime and quantum yield of the five complexes are recorded in aqueous medium and the increase in the number of antenna has also increased the quantum yield, and so does the overall absorption coefficients. (Table 2)

Low-temperature (77K) emission spectra of water-soluble gadolinium and europium complexes (Ln-1L; Ln-o-2L; Ln-p-2L; Ln-3L and Ln-4L, Ln = Gd or Eu)

The energy difference in the levels between the triplet state of the organic antenna and the excited state of lanthanide ion is critical for the emission efficiency. There are lots of studies in the literature showing that the optimum energy gap should be between 2000 and 5000 cm^{-1}.[17] However, there are limited studies on the increased number of the antenna in the same coordinated skeleton to the lanthanide. Five gadolinium motif complexes had been synthesized and their triplet state of antenna had been determined with their phosphorescence spectra at 77K. The lowest energy level of Gd^{3+} ($^6P_{7/2}$) is much higher than energy levels of the ligands; therefore, it is assumed that there is no energy transition between the ligand and metal.[18] The phosphorescence of these Gd complexes was measured under cold conditions (77 K) in the mixture of H_2O: glycerol (Fig. 6). The luminescence lifetimes were recorded to verify the fluorescence and phosphorescence at 77K (Table 3). The emission lifetimes on a nanosecond scale ($S_1 \rightarrow S_0$) were measured at ca. 430 nm for ligands in five complexes, respectively, and on a microsecond scale ($T_1 \rightarrow S_0$) at ca. 460 to 470 nm for ligands in five complexes, respectively. All the triplet states of ligands in five complexes are within 2000-5000 cm^{-1} compared with the 1st excited state of $^5D_0$ in europium, and are appropriate for the energy transfer to europium from ligand for f-f emission. It is impossible to identify the o- and p-isomerism of europium complexes with two antenna by mass and UV-Vis absorption spectroscopy. The ^{1}H NMR spectrum is only available for the symmetrical p-isomer (Fig. 3). The hypersensitive and fingerprint emission band of europium in this case can help to identify the o- and p- isomers. In the room temperate emission spectra of Eu-o-2**L**, the ratio of $^5D_0$ to ^7F_J, (J = 1, 2 and 4) is 1:1.89:2.92 but for Eu-p-2**L**, the ratio is 1:1.15:1.73 (Fig. 5 and Table 1). The spectral features are only partially resolved at room temperature. In order to gain a clearer distinction between Eu-o-2**L** and Eu-p-2**L**, the high resolution low temperature (77 K) spectra of these two complexes were obtained. As shown in Fig. 7, all electric dipole and magnetic transition with crystal splitting are well defined. The major difference in the 77 K spectra compared with the room temperature spectra is the smaller relative intensity of the $^5D_0 \rightarrow {}^7F_0$ transition for both Eu-o-2**L** and Eu-p-2**L**, which may indicate changes in the Eu^{3+} site symmetry or less thermal disorder. Greater noise level can be found in Eu-p-2**L** and spectral feature of for Eu-p-2**L** is slightly blue shift relative to those in Eu-o-2**L** (i.e. $^5D_0 \rightarrow {}^7F_0$ transition for Eu-o-2**L**, 17218 cm^{-1} and in Eu-p-2**L** is 17226 cm^{-1}). The most prominent $^5D_0 \rightarrow {}^7F_1$ transition bands are at 591.2 and 594.9 nm

for Eu-o-2**L**, whereas for Eu-p-2**L**, there are four emission bands located at 590, 592.4, 597.6 and 600 nm. For Eu-o-2**L**, two bands are observed for the $^5D_0 \rightarrow {}^7F_1$ transition region. This could be a consequence of the resonance coupling of the excited-state electronic crystal-field levels with low-energy vibrational excitations of the electronic ground state. However, for Eu-p-2**L**, it seems that there are two set of $^5D_0 \rightarrow {}^7F_1$ transition bands and similar observations have been found in $^5D_0$ to $^7F_4$ transitions for Eu-p-2**L**. This should be induced by the presence in solution of a mixture of two distinct coordination environment associated with the square antiprismic and twisted square antiprismic isomers.[19] From Fig. 7, a clear distinction of isomers Eu-o-2**L** and Eu-p-2**L** from their emission spectra could be achieved. In view of the presence of more than $2J + 1$ bands for the $^5D_0 \rightarrow {}^7F_{1,2}$ transitions for both Eu-o-2**L** and Eu-p-2**L**, especially in Eu-p-2**L**, the spectra illustrate the possibility of square antiprismic and twisted square antiprismic isomers; however, to carry out a crystal-field analysis of the energy levels here is far beyond the scope of this study and thus would not be attempted here.

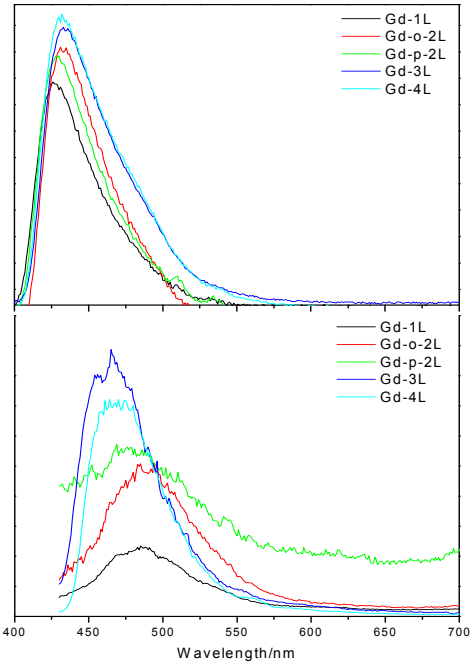

Fig. 6 Fluorescence (upper, 298K) and phosphorescence (lower, 77K) spectra of antenna in five water-soluble gadolinium complexes. (Motif structures of five europium complexes in Fig. 1)

Table 3. The emission bands and lifetimes (bracket, μs) of five gadolinium complexes (Gd-1**L**; Gd-o-2**L**; Gd-p-2**L**; Gd-3**L** and Gd-4**L**) at 298K and 77 K (λ_{ex} = 330 nm).

	Gd-1**L**	Gd-o-2**L**	Gd-p-2**L**	Gd-3**L**	Gd-4**L**
298K	23365 (0.017)	23041 (0.021)	23474 (0.018)	22989 (0.025)	23095 (0.026)
77K	20619 (0.101)	20450 (0.110)	21097 (0.103)	21231 (0.116)	21368 (0.125)

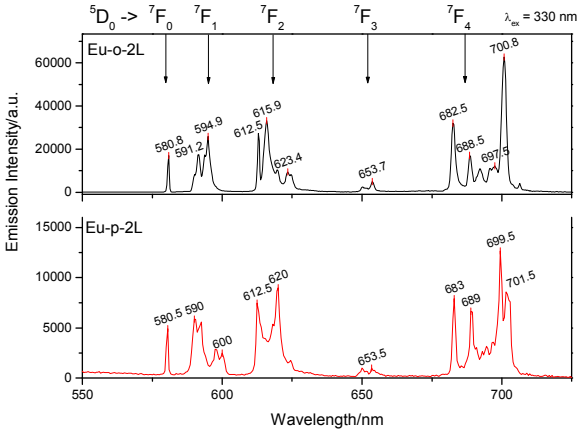

Fig. 7 77K Emission spectra of Eu-p-2**L** and Eu-o-2**L** in aqueous solution, 1 μM. (λ_{ex} = 330 nm)

In vitro studies of the five water-soluble europium complexes

With the aim to further develop time-resolved imaging probes using the five complexes, the subcellular uptake profile (amounts and localization) and cytotoxicity of them have to be evaluated via inductively coupled plasma mass spectroscopy (ICP-MS), 3-(4, 5-dimethylthiazol-2-yl)-2 and 5-diphenyltetrazolium bromide (MTT) assay and in vitro imaging (with co-staining commercial available marker). From the cellular uptake profile, one can see that Eu-4**L** (+3) and Eu-3**L** (+2) have shown a higher uptake amount than the other three in HeLa (human cervical carcinoma cell line) cells by checking the europium content inside the cells via ICP-MS (Fig. 8). For Eu-o-2**L** and Eu-p-2**L**, the overall charge is the same, in addition to the molecular weight and the antenna, but the uptake profiles are different as shown in the emission spectra in Fig. 9. As a potential time resolved imaging marker, the dark toxicity of each has also to be evaluated. The MTT assays of five water-soluble europium complexes had been done in HeLa cells. The half maximal inhibitory concentration (IC_{50}) of these complexes in HeLa cells are around 0.5 mM for Eu-1**L**; Eu-p-2**L**; and Eu-4**L**, Eu-o-2**L**, while Eu-3**L** is ~0.25 mM. The uptake amount of Eu-p-2**L** is greater than Eu-o-2**L**. Less steric hindrance may improve the cellular uptake rate in vitro. Even the uptake of Eu-p-2**L** is much greater than Eu-o-2**L**, Eu-p-2**L** has shown much higher toxicity than Eu-o-2**L** (Fig. 8c). The IC_{50} value of Eu-o-2**L** in HeLa cells is 0.5 mM, but Eu-p-2**L** is ~0.23 mM. All five europium complexes are soluble in water and are localized in the cytoplasm, except for Eu-4**L**. The pale red emission can be observed for Eu-1**L**; Eu-o-2**L**; Eu-p-2**L** in HeLa cells (Fig. 9). Eu-3**L** and Eu-4**L** have strong emission in water (Fig. 9d and e). After 3-hour incubation time of 1 μM Eu-4**L** in HeLa cells, the red emission of Eu-4**L** can be observed in the lysosome of HeLa cells. This subcellular localization has been further confirmed with the co-staining with the green lysotracker (Fig. 9i).

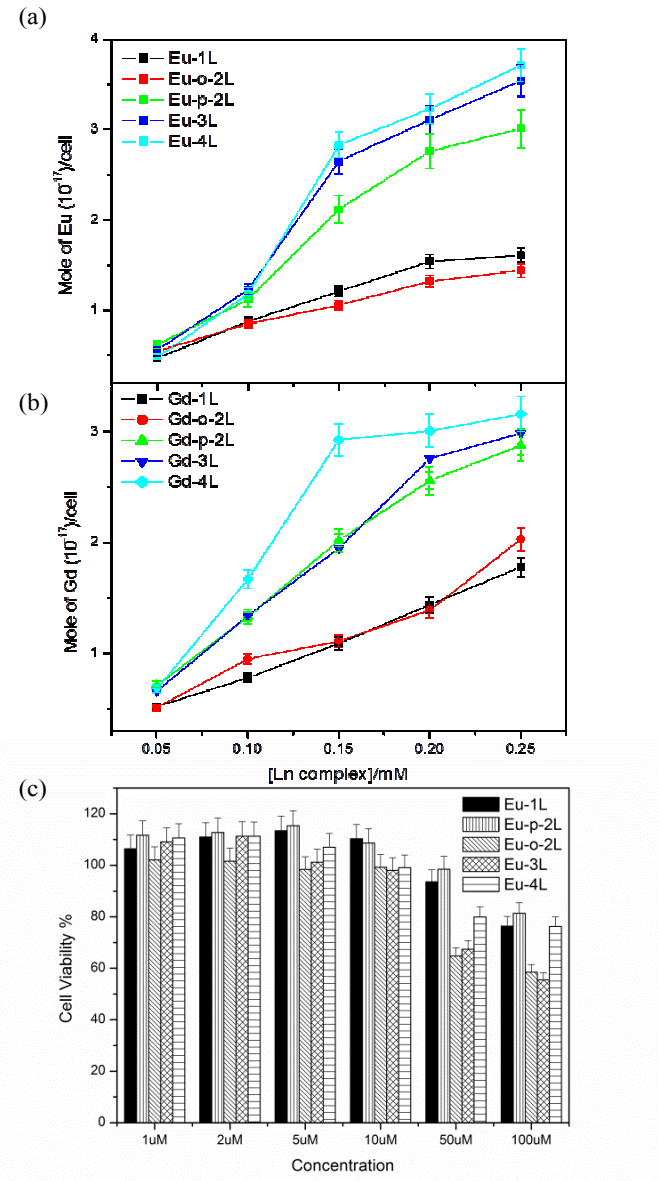

Fig. 8 (a) and (b) The subcellular uptake evaluation via ICP-MS and (c) the dark cytotoxicity of five water-soluble europium complexes in HeLa cells with various dosed concentrations.

Conclusions

In conclusion, we had synthesized five water-soluble, cyclen-based europium complexes with various numbers of the same antenna, 2-methyl-4-(2-(4-propoxyphenyl)-ethynyl)pyridine (**L**). Full characterizations of them had also been achieved with various spectroscopic techniques that Eu-3**L** with an overall positively doubly charge was found to be the best energy-transfer sensitization system, while Eu-4**L** exhibited the most impressive europium emission quantum yield in aqueous solution (~16%). Per a series of in vitro studies, it is our Eu-4**L** that are non-cytotoxic, cell-permeable, and in particular lysosome-selective that holds great promise for further development.

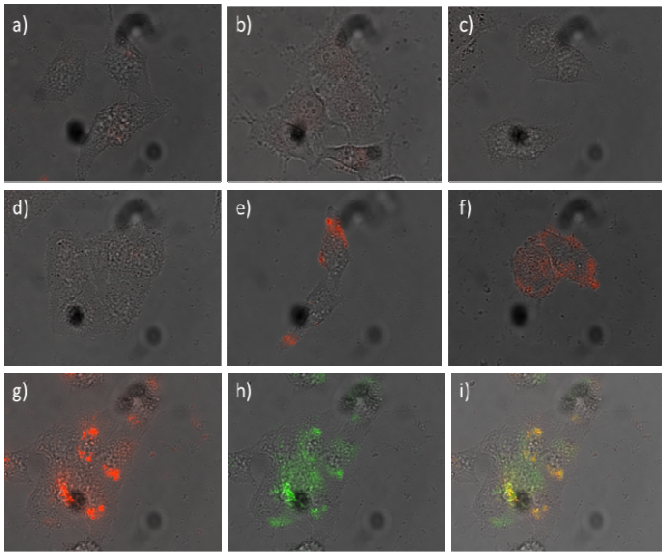

Fig. 9 In vitro imaging of five water-soluble europium complexes in HeLa cell with 3-hour incubation (λ_{ex} = 405 nm). a) Eu-1**L** (24 hours); b) Eu-o-2**L** (24 hours); c) Eu-p-2**L** (24 hours); d) Eu-3**L** (24 hours); e) Eu-4**L** (3 hours); f) Eu-4**L** (**6** hours); g) Eu-4**L** (24 hours); h) Lyso Tracker; i) Eu-4**L** + Lyso Tracker.

Experimental Section

Synthesis

General information. All air and water sensitive reactions were carried out under a nitrogen atmosphere with dry solvents under anhydrous conditions unless otherwise noted. All the chemicals were purchased commercially and used without further purification. Anhydrous THF and toluene were distilled from sodium-benzophenone, and dichloromethane was distilled from calcium hydride. Yields refer to chromatographically treated quantities, unless otherwise stated. Reactions were monitored by thin-layer chromatography (TLC) carried out on 0.25 mm silica gel plates (60F-254) that were analyzed by staining with $KMnO_4$ (200 mL H_2O of 1.5 g $KMnO_4$, 10 g K_2CO_3 and 1.25 mL of 10% aqueous NaOH). Fluorescence was triggered upon 254 nm irradiation or by staining with anisaldehyde (450mL of 95% EtOH, 25 mL of conc.H_2SO_4, 15mLof acetic acid, and 25 mL of anisaldehyde). Silica gel (60, particle size 0.040–0.063 mm) was used for flash chromatography. IR spectra were obtained using FT-IR Spectrometer, whereas NMR spectra were recorded on either a 400 (^{1}H: 400 MHz, ^{13}C: 100 MHz), or 500 (^{1}H: 500 MHz, ^{13}C: 125 MHz). The following abbreviations were used to explain the multiplicities: s = singlet, d = doublet, t = triplet, q = quartet, m = multiplet, b = broad. High-resolution mass spectra were obtained from a MALDI-TOF Mass Spectrometer. Melting points were uncorrected and determined on a micro-melting point meter.

Compound **2**. To a stirred solution of **1** (800 mg, 3.0 mmol) and Et_3N (910 mg, 9.0 mmol) in CH_2Cl_2 (30 mL) at room temperature, methanesulfonyl chloride (517 mg, 4.5 mmol) was added dropwise. After stirring at room temperature for 20 minutes, the reaction was quenched by the addition of a

saturated $NaHCO_3$ solution (30 mL). The organic phase was separated, dried over $MgSO_4$, filtered, and concentrated. To a stirred solution of the crude product in acetone (30 mL) at room temperature LiBr (6.0 mmol) was added. The resulting mixture was stirred at 60 ºC for 2 hours and then concentrated. The residue was dissolved in water (30 mL) and extracted with CH_2Cl_2 (3×30 mL). The combined organic layers were dried over $MgSO_4$, filtered, and concentrated. Silica gel flash column chromatography (hexane/ethyl acetate; 15/1 to 10/1 to 8/1) of the residue gave a white solid (710 mg, 72%) as the product. **2**: R_f = 0.75 (silica gel, hexane/ethyl acetate = 8:1); ^{1}H NMR (400 MHz, $CDCl_3$) δ 8.55 (d, *J* = 7 Hz, 1H), 7.48 (s, 1H), 7.50 (d, *J* = 7 Hz, 2H), 7.28 (d, *J* = 7 Hz, 1H), 6.91 (d, *J* = 7 Hz, 1H), 4.67 (s, 2H), 3.96 (t, *J* = 7 Hz, 2H), 1.88-1.78 (m, 2H), 1.05 (t, *J* = 7 Hz, 3H); ^{13}C NMR (100 MHz, $CDCl_3$) δ 160.1, 156.6, 149.3, 133.5, 133.2, 124.6, 124.5, 114.7, 113.7, 95.11, 85.4, 69.6, 46.4, 22.5, 10.5; HRMS (ESI) m/z calcd. for $C_{17}H_{17}BrNO$ $(M+H)^+$ 330.0494, found 330.0451.

Compound 1**L**. To a degassed solution of **2** (80 mg, 0.24 mmol) in MeCN (15 mL) at room temperature, K_2CO_3 (92 mg, 1.21 mmol) and DO3A(O*t*Bu)$_3$ (123 mg, 0.24 mmol) were added. The resulting mixture was stirred at 80 ºC for 6 hours and then quenched by addition of water (15 mL). The aqueous solution was extracted with CH_2Cl_2 (3×15 mL). The combined organic layers were dried over $MgSO_4$, filtered, and concentrated. Silica gel flash column chromatography (CH_2Cl_2/MeOH; 25/1 to 20/1 to 10/1) of the residue gave an off-white oil (124 mg, 68%) as the product. 1**L**: R_f = 0.42 (silica gel, CH_2Cl_2/MeOH = 10:1); ^{1}H NMR (500 MHz, $CDCl_3$) δ 8.20 (d, *J* = 7 Hz, 1H), 7.44 (d, *J* = 7 Hz, 2H), 7.24 (s, 1H), 7.17 (d, *J* = 7 Hz, 1H), 6.86 (d, *J* = 7 Hz, 2H), 3.93 (t, *J* = 7 Hz, 2H), 3.57 (s, 2H), 3.21-2.30 (m, 22H), 1.80-1.76 (m, 2H), 1.46 (s, 18H), 1.38 (s, 9H), 1.05 (t, *J* = 7 Hz, 3H); ^{13}C NMR (125 MHz, $CDCl_3$) δ 172.7, 172.4, 160.1, 158.8, 148.6, 133.4, 132.8, 124.9, 123.6, 114.7, 113.5, 95.1, 85.2, 81.9, 81.8, 69.6, 58.7, 56.3, 55.5, 53.3, 50.3, 27.9, 22.4, 10.3; HRMS (ESI) m/z calcd. for $C_{43}H_{66}N_5O_7$ $(M+H)^+$ 764.4962, found 764.4961.

Compound o-2**L**. To a degassed solution of **2** (80 mg, 0.24 mmol) in MeCN (15 mL) at room temperature, K_2CO_3 (166 mg, 1.21 mmol) and DO2A-*o*-(O*t*Bu)$_2$ (48 mg, 0.12 mmol) were added. The resulting mixture was stirred at 80 ºC for 6 hours and then quenched by addition of water (15 mL). The aqueous solution was extracted with CH_2Cl_2 (3×15 mL). The combined organic layers were dried over $MgSO_4$, filtered, and concentrated. Silica gel flash column chromatography (CH_2Cl_2/MeOH; 25/1 to 20/1 to 10/1) of the residue gave an off-white oil (67 mg, 62%) as the product. o-2**L**: R_f = 0.45 (silica gel, CH_2Cl_2/MeOH = 10:1); ^{1}H NMR (400 MHz, $CDCl_3$) δ 7.53 (d, J = 7 Hz, 2H), 7.43 (d, J = 7 Hz, 4H), 7.22 (s, 2H), 7.11 (s, 2H), 6.86 (d, J = 7 Hz, 4H), 3.93 (t, J = 7 Hz, 4H), 3.50 (s, 4H), 3.21-2.30 (m, 20H), 1.80-1.74 (m, 4H), 1.42 (s, 18H), 1.02 (t, J = 7 Hz, 6H); ^{13}C NMR (75 MHz, CD_3OD) δ 172.9, 160.7, 160.3, 159.1, 159.0, 148.8, 133.2, 132.8, 125.0, 123.4, 114.5, 113.4, 94.5, 84.8, 81.8, 69.3, 58.5, 55.8, 55.2, 50.3, 49.9, 27.1, 22.1, 9.4; HRMS (ESI) m/z calcd. for $C_{54}H_{71}N_6O_6$ $(M+H)^+$ 899.5435, found 899.5432.

Compound p-2**L**. To a degassed solution of **2** (80 mg, 0.24 mmol) in MeCN (15 mL) at room temperature, K_2CO_3 (166 mg, 1.21 mmol) and DO2A-*p*-(O*t*Bu)$_2$ (48 mg, 0.12 mmol) were added. The resulting mixture was stirred at 80 ºC for 6 hours and then quenched by addition of water (15 mL). The aqueous solution was extracted with CH_2Cl_2 (3×15 mL). The combined organic layers were dried over $MgSO_4$, filtered, and concentrated. Silica gel flash column chromatography (CH_2Cl_2/MeOH; 25/1 to 20/1 to 10/1) of the residue gave an off-white oil (80 mg, 75%) as the product. p-2**L**: R_f = 0.45 (silica gel, CH_2Cl_2/MeOH = 10:1); ^{1}H NMR (400 MHz, $CDCl_3$) δ 8.34 (d, *J* = 7 Hz, 2H), 7.48 (d, *J* = 7 Hz, 4H), 7.29 (s, 2H), 7.21 (d, *J* = 7 Hz, 2H), 6.90 (d, *J* = 7 Hz, 4H), 3.96 (t, *J* = 7 Hz, 4H), 3.52 (s, 4H), 3.21-2.30 (m, 20H), 1.84-1.79 (m, 4H), 1.33 (s, 18H), 1.05 (t, *J* = 7 Hz, 6H); ^{13}C NMR (100 MHz, $CDCl_3$) δ 171.9, 160.1, 158.6, 149.1, 133.5, 132.8, 125.0, 123.7, 114.7, 113.5, 95.2, 85.3, 81.8, 69.7, 58.7, 56.9, 50.3, 28.0, 22.5, 10.5; HRMS (ESI) m/z calcd. for $C_{54}H_{71}N_6O_6$ $(M+H)^+$ 899.5435, found 899.5427.

Compound 4**L** and **6**. To a degassed solution of **2** (240 mg, 0.72 mmol) in MeCN (25 mL) at room temperature, K_2CO_3 (500 mg, 3.63 mmol) and cyclen (35 mg, 0.20 mmol) were added. The resulting mixture was stirred at 80 ºC for 6 hours and then quenched by addition of water (25 mL). The aqueous solution was extracted with CH_2Cl_2 (3×25 mL). The combined organic layers were dried over $MgSO_4$, filtered, and concentrated. Silica gel flash column chromatography (CH_2Cl_2/MeOH; 25/1 to 20/1 to 10/1) of the residue gave two off-white oils 4**L** (105 mg, 45%) and **6** (55 mg, 30%) as the major products. 4**L**: R_f = 0.71 (silica gel, CH_2Cl_2/MeOH = 10:1); ^{1}H NMR (400 MHz, $CDCl_3$) δ 7.53 (d, *J* = 7 Hz, 4H), 7.47 (d, *J* = 7 Hz, 8H), 7.20 (s, 4H), 7.08 (d, *J* = 7 Hz, 4H), 6.90 (d, *J* = 7 Hz, 8H), 3.96 (t, *J* = 7 Hz, 8H), 3.41-2.30 (m, 24H), 1.86-1.79 (m, 8H), 1.06 (t, *J* = 7 Hz, 12H); ^{13}C NMR (125 MHz, $CDCl_3$) δ 160.2, 158.9, 148.8, 133.5, 132.8, 125.4, 123.9, 114.8, 113.5, 95.4, 85.1, 69.7, 59.0, 50.4, 22.4, 10.3; HRMS (ESI) m/z calcd. for $C_{76}H_{81}N_8O_4$ $(M+H)^+$ 1169.6383, found 1169.6373. **6**: R_f = 0.50 (silica gel, CH_2Cl_2/MeOH = 10:1); ^{1}H NMR (400 MHz, $CDCl_3$) δ 7.53 (d, *J* = 7 Hz, 3H), 7.48 (d, *J* = 7 Hz, 6H), 7.19 (s, 3H), 7.08 (d, *J* = 7 Hz, 3H), 6.90 (d, *J* = 7 Hz, 6H), 3.96 (t, *J* = 7 Hz, 6H), 3.41-2.30 (m, 22H), 1.86-1.79 (m, 6H), 1.06 (t, *J* = 7 Hz, 9H); ^{13}C NMR (125 MHz, $CDCl_3$) δ 160.3, 158.7, 148.9, 133.5, 132.8, 125.4, 123.9, 114.8, 113.5, 95.4, 85.1, 69.6, 58.7, 50.4, 48.5, 47.6, 22.4, 10.3; HRMS (ESI) m/z calcd. for $C_{59}H_{66}N_7O_3$ $(M+H)^+$ 920.5229, found 920.5212.

Compound 3**L**.: To a degassed solution of **6** (30 mg, 0.03 mmol) in MeCN (10 mL) at room temperature, K_2CO_3 (69 mg, 0.5 mmol) and *t*-butyl 2-bromoacetate (19 mg, 0.10 mmol) were added. The resulting mixture was stirred at 80 ºC for 6 hours and then quenched by adding water (10 mL). The aqueous solution was extracted with CH_2Cl_2 (3×10 mL). The combined organic layers were dried over $MgSO_4$, filtered, and concentrated. Silica gel flash column chromatography (CH_2Cl_2/MeOH; 25/1 to 20/1 to 10/1) of the residue gave an-off white oil (28 mg, 89%) as the product. 3**L**: R_f = 0.62 (silica gel, CH_2Cl_2/MeOH = 10:1); ^{1}H NMR (500 MHz, $CDCl_3$) δ 7.53 (d, *J* = 7 Hz, 3H), 7.48 (d, *J* = 7 Hz, 6H), 7.26 (d, *J* = 7 Hz, 3H), 7.05 (d, *J* = 7 Hz, 3H), 6.90 (d, *J* = 7 Hz, 6H), 3.96 (t, *J* = 7 Hz, 6H), 3.46, (s, 6H), 3.41-2.30 (m, 18H), 1.86-1.79 (m, 6H), 1.38 (s, 9H), 1.06 (t, *J* = 7 Hz, 9H); ^{13}C NMR (125 MHz, $CDCl_3$) δ 160.2, 158.7, 148.9, 148.7, 133.5, 132.8, 125.4, 123.9, 114.8, 113.5, 95.4, 85.2, 85.1, 81.8, 69.6, 59.2, 58.8, 56.9, 50.3, 28.0, 22.4, 10.4; HRMS (ESI) m/z calcd. for $C_{65}H_{76}N_7O_5$ $(M+H)^+$ 1034.5910, found 1034.5906.

General procedures for Ln (Eu, Gd) complexes Ln-*n***L** (*n*=1, o-2, p-2, 3): Ligand L*n* (*n*=1, o-2, p-2, 3) (0.020 mmol) were

dissolved in TFA (1 mL) and the mixture was stirred at room temperature under argon for 12 hours. After removal of TFA under reduced pressure, the pale yellow residue was dissolved in CH_2Cl_2, and concentrated to ensure the removal of TFA. Deprotection of the ^{t}Bu groups was confirmed by ^{1}H NMR of the crude product. The residue was then dissolved in H_2O/MeOH (2:1 v/v, 3 mL) and treated with $EuCl_3{\cdot}(H_2O)_6$ or $GdCl_3$ (0.020 mmol). After adjustment of the pH to 7.0 with an 1 N aqueous sodium hydroxide solution, the mixture was stirred at 70 ℃ for 24 hours. Concentration and recrystallization of the crude product from CH_3CN gave an off-white solid as the product. Eu-1**L**: 75% yield; ^{1}H NMR (500 MHz, CD_3OD) δ 28.21, 27.50, 24.27, 13.01, 11.78, 10.09, 7.01-9.27, 4.02, 1.81, 1.09, -1.71, -3.78, -5.12, -7.50, -8.10, -8.72, -10.10, -11.21, -12.02, -12.60, -15.01, -16.28, -17.50, -21.02, -22.47; HRMS (ESI) m/z calcd. for $C_{31}H_{41}EuN_5O_8$ $(M+H_2O+H)^+$764.2167, found 764.2221, $(M+H)^+$746.2062, found 746.2051; t_R (retention time for HPLC) = 10.48min; IR (neat, 298K, cm^{-1}) 3223.20, 2877.79, 1585.49, 1411.89, 1321.24, 1253.73, 1176.58, 1082.07, 1006.84, 947.05, 839.03, 798.53; mp > 320 ºC; [Eu-p-2**L**]Cl: 73% yield; ^{1}H NMR (500 MHz, CD_3OD) δ 24.50, 23.62, 13.21, 14.09, 9.51, 9.27, 9.10, 8.17, 7.62, 7.40, 7.12, 4.37, 4.02, 1.81, 1.02, -2.21, -3.75, -5.91, -7.50, -11.72, -12.52, -16.07, -18.23, -21.10, -25.71; HRMS (ESI) m/z calcd. for $C_{46}H_{53}ClEuN_6O_6$ $(M+H_2O+H)^+$991.3035, found 991.2779, $(M+H)^+$973.2927, found 973.3058; t_R (retention time for HPLC) = 10.93min; IR (neat, 298K, cm^{-1}) 3176.67, 3099.61, 2879.72, 1639.49, 1371.38, 1259.52, 1172.72, 1082.07, 999.13, 974.05, 833.25, 567.07; mp > 320 ºC; [Eu-o-2**L**]Cl: 73% yield; ^{1}H NMR (500 MHz, CD_3OD) δ 18.60, 14.79, 15.02, 9.57, 9.21, 9.07, 8.02, 7.57, 7.10, 4.02, 1.82, 1.07, -2.25, -3.90, -5.01, -7.50, -10.01, -11.70, -12.54, -14.22, -15.09, -18.29; HRMS (ESI) m/z calcd. for $C_{46}H_{53}ClEuN_6O_6$ $(M+H_2O+H)^+$991.3035, found 991.2933, $(M+H)^+$973.2927, found 973.2929; t_R (retention time for HPLC) = 11.04min; IR (neat, 298K, cm^{-1}) 3334.92, 3174,83, 2943.37, 2879.72, 2362.80, 2227.78, 1417.68, 1327.03, 1207.44, 1143.79, 1080.14, 974.05, 796.60, 605.65; mp > 320 ºC; [Eu-3**L**]Cl_2: 80% yield; ^{1}H NMR (500 MHz, CD_3OD) δ 31.07, 25.23, 24.09, 13.12, 11.03, 10.18, 9.57, 9.10, 8.59, 7.52, 7.21, 5.13, 4.01, 1.82, 1.07, -3.09, -5.10, -6.92, -7.83, -8.90, -10.11, -11.70, -15.28, -20.13, -21.95; HRMS (ESI) m/z calcd. for $C_{62}H_{67}Cl_2EuN_7O_5$ $(M+H_2O+H)^+$1218.3899, found 1218.4003, $(M+H)^+$1200.3793, found 1200.3915; t_R (retention time for HPLC) = 10.62min; IR (neat, 298K, cm^{-1}) 3336.85, 2943.37, 2227.78, 1624.06, 1207.44, 1145.72, 1010.70, 796.60, 601.79, 487.99; mp > 320 ºC; Gd-1**L**: 70% yield; HRMS (ESI) m/z calcd. for $C_{31}H_{41}GdN_5O_8$ $(M+H_2O+H)^+$769.2196, found 769.2229, (M+H2O+Na)$^+$: 791.2016, found 791.2047. [Gd-p-2**L**]Cl: 78% yield; HRMS (ESI) m/z calcd. for $C_{46}H_{53}ClGdN_6O_6$ $(M+H)^+$978.2956, found 978.3188. [Gd-o-2**L**]Cl: 72% yield; HRMS (ESI) m/z calcd. for $C_{46}H_{53}ClGdN_6O_6$ $(M+H)^+$978.2956, found 978.3176. [Gd-3**L**]Cl_2: 81% yield; HRMS (ESI) m/z calcd. for $C_{62}H_{67}Cl_2EuN_7O_5$ $(M+H)^+$ 1205.3822, found 1205.4015.

Ln complex Ln-4**L** (Ln = Eu, Gd). Ligand 4**L** (0.040 mmol) was dissolved in MeCN and treated with $EuCl_3{\cdot}(H_2O)_6$ or $GdCl_3$ (0.040 mmol). The mixture was stirred at 70 ℃ for 24 hours. Concentration and recrystallization of the crude product from CH_3CN gave an off-white solid as the product. [Eu-4**L**]Cl_3: 88% yield; ^{1}H NMR (500 MHz, CD_3OD) δ 15.02, 3.99, 1.82, 1.06, -0.33, -6.49, -7.81, -8.22, -13.31, -14.06, -16.47; HRMS (ESI) m/z calcd. for $C_{76}H_{80}Cl_2EuN_8O_4$ $(M-Cl)^+$1391.4892, found 1391.4657; $C_{76}H_{80}ClEuN_8O_4$ $(M-2Cl)^{2+}$ 678.2569, found 678.2497, $(M-3Cl)^{3+}$ 440.5172, found 440.5215; t_R (retention time for HPLC) = 11.33min; IR (neat, 298K, cm^{-1}) 3381.21, 2935.66, 2875.86, 2204.64, 1514.12, 1249.87, 1172.72, 1004.91, 933.55, 831.32, 553.57, 540.07; mp > 320 ºC; [Gd-4**L**]Cl_3: 85% yield; HRMS (ESI) m/z calcd. for $C_{76}H_{80}Cl_2GdN_8O_4$ $(M-Cl)^+$1396.4921, found 1396.4465; $C_{76}H_{80}ClGdN_8O_4$ $(M-2Cl)^{2+}$680.7611, found 680.7364.

Photophysical properties of the lanthanide complexes

UV-Visible absorption spectra in the spectral range 200 to 1100 nm were recorded by an HP UV-8453 spectrophotometer. Single-photon luminescence spectra were recorded using an Edinburgh Instrument FLS920 Combined Fluorescence Lifetime and Steady state spectrophotometer that was equipped with a red sensitive single photon counting photomultiplier by Peltier Cooled Housing. The spectra were corrected for detector response and stray background light phosphorescence. The quantum yields of the compounds were measured by Demountable 142mm (inner) diameter barium sulphide-coated integrating sphere supplied with two access ports. Low-temperature (77 K) phosphorescence spectra were obtained by exciting samples with a xenon lamp. The transparent glassy materials were formed by mixing samples with 2-methyltetrahydrofuran. The samples were placed in a tailor-made quartz tube housed in an Oxford Instruments liquid nitrogen cryostat.

The sensitization efficiencies of the Eu^{3+} $^5D_0$ luminescent state, η_{sens}, in five europium complexes are related to the overall quantum yield upon ligand excitation, Q_{Eu}^L, which we have determined by the integrating sphere method and by the following equation:[12], [14]-[15]

$$Q_{\mathrm{Eu}}^{\mathrm{L}} = \eta_{\mathrm{sens}} Q_{\mathrm{Eu}}^{\mathrm{Eu}} = \eta_{\mathrm{sens}} \tau_{\mathrm{obs}} / \tau_{\mathrm{rad}}$$

where Q_{Eu}^{Eu} represents the intrinsic quantum yield (i.e. employing direct excitation into Eu^{3+} energy levels); τ_{obs} and τ_{rad} are the observed and radiative (or natural) lifetimes of the $^5D_0$ state. The latter can be estimated if the spontaneous emission probability in vacuo of the magnetic dipole allowed $^5D_0 \rightarrow {}^7F_1$ transition is assumed to be constant (i.e. 14.65 s^{-1}), with constant energy for the transition. This value needs to be corrected by the (cube of the) refractive index of the water and taking the value 1.333 gives the radiative lifetime of the $^5D_0 \rightarrow {}^7F_1$ transition as 19.51 ms. The radiative lifetime of the $^5D_0$ state (in ms) may then be estimated by the comparison of integrated areas, I, as follows:[12], [14]-[15]

$$(\tau_{\mathrm{rad}})^{-1} = [I_{\mathrm{TOT}} / I_{^5\mathrm{D}_0 \rightarrow {}^7\mathrm{F}_1}] / 16.7$$

where I_{TOT} denotes the entire area of the $^5D_0 \rightarrow {}^7F_J$ transitions. Thus, from measurements of $^5D_0$ lifetime (τ_{obs}), overall quantum efficiency, Q_{Eu}^L, and integrated spectral areas, it is possible to estimate the sensitization efficiency (η_{sens}) of Eu^{3+} $^5D_0$ luminescence by the coordinated ligands.

pKa values[20]

The pH of the solution was carefully controlled to the designated pH according to the follow usual Tris buffer (pH 2-12) protocol. The pH was monitored using a Mettler Toledo DT120 glass electrode equipped with a temperature sensor (PT100, class B). This electrode was operated through a Mettler

Toledo MP120 pH meter, which was calibrated using standard buffer solutions of pH=7.0. The pH dependent luminescent intensity profile of europium complexes (10 μM) was obtained by monitoring the emission intensity at 615 nm at each point (1.0 pH value per titration interval from 2.0−14.0, see Fig. S8 in the supporting information). The apparent protonation constants were calculated from the data obtained following these luminescent titrations. The equation shown below was fitted to the data, using a nonlinear least squares fitting algorithm:

$$[X] = \frac{f/K + [EuL]^* f - [EuL]^* f^2}{1-f} \quad \text{Wherein,} \quad f = \frac{F - F_0}{F_1 - F_0}$$

[X] is the concentration of the anion or selected added species in solution; K is the apparent protonation constant; F is the ratio or intensity of the selected peak; F_0 is the ratio or intensity of the selected peak at the beginning of the titration; F_1 is the final ratio or intensity of the selected peak; [LnL] is the total concentration of the Ln(III) complex in solution.

Tris buffer (pH 2-12) Protocol

1. Base Solution: 0.1 M citric acid (21.01 g/L), 0.1 M KH_2PO_4 (13.61 g/L), 0.1 M sodium tetraborate (19.07 g/L), 0.1 M Tris (12.11 g/L), 0.1 M KCl (7.46 g/L) in 50 mL distilled water.
2. Add *x* mL of 0.4 M HCl or 0.4 M NaOH to adjust desired pH value

pH (25°C)	*x*	additive
2	34.8	0.4 M HCl
3	19.6	
4	10.0	
5	0.4	0.4 M NaOH
6	11.4	
7	22.4	
8	33.2	
9	46.2	
10	59.0	
11	65.6	
12	77.2	

3. Dilute to 200 mL with mQ water

HPLC analysis

The reverse-phase HPLC analysis of these five europium complexes was carried out at room temperature by using an Agilent ZORBAX SB-C18 Stable Bond Analytical 4.6 X 150 mm 5-micron column. The mobile phase is 0.1% formic acid in mQ water and 0.1% formic acid in MeCN solvent system, and the flow rate is 1.0 mL/min. Solvent gradient program is listed in the following Table.

Time /min	0.1% CHOOH in mQ water /%	0.1% CHOOH in CH_3CN /%
0.0	95	5
14.0	50	50
15.0	50	50
20.0	0	100

In vitro studies

Cell culture

Human cervical carcinoma HeLa cells were purchased from the American type Culture Collection (ATCC) (#CCL-185, ATCC, Manassas, VA, USA). The HeLa cells were grown in Dulbecco's Modified Eagle Medium (DMEM) supplemented with 10 % fetal bovine serum (FBS), 1 % penicillin and streptomycin at 37 ºC, and 5 % CO_2. To apply europium complexes for fluorescence imaging, HeLa cells were incubated in DMEM containing 1 to 5 L complexes at 37 ºC for 24 hours under 5% CO_2, and then washed with Phosphate-buffered saline (PBS) to remove excess complexes completely.

In vitro imaging

To test the suitability of the five water-soluble europium complexes as bioprobes, in vitro imaging of HeLa cells incubated with five complexes was performed on a commercial confocal laser scanning microscope, Leica TCS SP5, equipped with a Ti: Sapphire laser (Libra II, Coherent). All samples were excited by a 980 nm wavelength laser.

MTT cell viability assay.

Cells treated with five water-soluble europium complexes for 24 hours were further incubated with MTT, 3-(4, 5-dimethylthiazol-2-yl)-2 and 5-diphenyltetrazolium bromide (0.5 mg/mL) for 4 hours, to produce formazan during cell metabolism. Then, formazan were thoroughly dissolved by dimethyl sulfoxide (DMSO), and the absorbances of solutions were measured in Bio-Rad iMark microplate reader (490 nm). Quadruplicates were performed. Data analysis and plotting were operated by the GraphPad Prism 5 software.

ICP-MS studies

To measure the intracellular concentration of the complexes, HeLa cells were plated in each well and incubated with the complexes with the concentration from 0.05 to 0.25 mM, which was the same as in vitro imaging. After co-incubation, the cell culture medium containing complexes was removed and the exposed cells were further washed with 1mL PBS for 3 times to remove complexes adhering to the outer cell membrane. Then the cells were trypsinized and dispersed into 1mL of culture medium. The exposed cells were collected by centrifugation at 1000rpm for 10 minutes and the cell pellet was digested in 100 μL of concentrated HNO_3 at 70 ºC for 3 hours. The cellular uptake of complexes was determined using an Agilent 7500 series of inductively coupled plasma mass spectroscopy (ICP-MS). All ICP experiments were performed in triplicate and values obtained were averaged. The concentration of Eu/Gd per cell was calculated by determining the concentration of Eu/Gd in the cell lysate by ICP-MS and then dividing it by the number of cells which counted by haematocytometer.

Acknowledgements

This work was funded by Peking University Shenzhen Graduate School (Key State Laboratory of Chemical Genomics open-project

fellowship program), and the grants from The Hong Kong Research Grants Council (HKBU 203013, HKPolyU 5032/11P), Hong Kong Baptist University (FRG 2/12-13/002), and Shenzhen Science and Technology Innovation Committee (KQTD201103).

Notes and references

[a] Laboratory of Chemical Genomics, School of Chemical Biology and Biotechnology, Peking University Shenzhen Graduate School, Shenzhen University Town, Xili, Shenzhen 518055, China; lizc@pkusz.edu.cn
[b] Department of Applied Biological and Chemical Technology, Hong Kong Polytechnic University, Hung Hum, Hong Kong SAR; bcwtwong@polyu.edu.hk; ga-lai.law@polyu.edu.hk
[c] Department of Chemistry, Hong Kong Baptist University, Hong Kong SAR; klwong@hkbu.edu.hk

1. P. A. Tanner, *Chem. Soc. Rev.*, 2013, **42**, 5090–5101.
2. G. Mancino, A. J. Ferguson, A. Beeby, N. J. Long, and T. S. Jones, *J. Am. Chem. Soc.*, 2005, **127**, 524–525.
3. S. V. Eliseeva, and J. C. Bünzli, *Chem. Soc. Rev.*, 2010, **39**, 189–227.
4. R. Carr, N. H. Evan, and D. Parker, *Chem. Soc. Rev.*, 2012, **41**, 7673–7626.
5. W. S. Lo, W. M. Kwok, G. L. Law, C. T. Yeung, C. T. L. Chan, H. L. Yeung, H. K. Kong, C. H. Chen, M. Murphy, K. L. Wong, and W. T. Wong, *Inorg. Chem.*, 2011, **50**, 5309–5311.
6. T. Zhang, X. Zhu, W. M. Kwok, C. T. L. Chan, H. L. Tam, W. K. Wong, and K. L. Wong, *J. Am. Chem. Soc.*, 2011, **50**, 20120–20122.
7. S. J. Butler, L. Lamarque, R. Pal, and D. Parker, *Chem. Sci.*, 2014, **5**, 1750–1756.
8. E. G. Moore, A. P. S. Samuel, and K. N. Raymond, *Acc. Chem. Res.*, 2009, **42**, 542–552.
9. D. Parker, J. W. Walton, L. Lamarque, and J. M. Zwier, *Eur. J. Inorg. Chem.*, 2010, **25**, 3961–3966.
10. Y. W. Yip, H. Wen, W. T. Wong, P. A. Tanner, and K. L. Wong, *Inorg. Chem.*, 2012, **51**, 7013–7015.
11. C. Li, and W. T. Wong, Tetrahedron, 2004, 60, 5595–5601.
12. P. Caravan, J. J. Ellison, T. J. McMurry, and R. B. Lauffer, *Chem. Rev.*, 1999, **99**, 2293–2352.
13. M. C. Heffern, L. M. Matosziuk, and T. J. Meade, *Chem. Rev.*, 2014, **114**, 4496−4539.
14. J. G. G. Bunzli, *Chem. Rev.*, 2010, **110**, 2729 – 2755.
15. S. Aime, M. Botta, M. Fasano, M. P. M. Marques, C. F. G. C. Geraldes, D. Pubanz and A. E. Merbach, *Inorg. Chem.*, **1997**, *36*, 2059-2068.
16. A. Beeby, I. M. Clarkson, R. S. Dickins, S. Faulkner, D. Parker, M. Woods, L. Royles, A. S. De Sousa, J. A. G. William, and M. Woods, *J. Chem. Soc. Perkin Trans. 2*, 1999, 493–504.
17. M. H. V. Werts, R. T. F. Jukes, and J. W. Verhoeven, *Phys. Chem. Chem. Phys.,* 2002, **4**, 1542–1548.
18. G. L. Law, K. L. Wong, K. K. Lau, H. L. Yam, K. W. Cheah, and W. T. Wong, *Eur. J. Inorg. Chem.*, 2007, **34**, 5419–5425.
19. H. Wen, C. K. Duan, G. Jia, P. A. Tanner, and M. G. Brik, *J. Appl. Phys.*, 2011, **110**, 033536–033538.
20. D. G. Smith, B. K. McMahon, R. Pal and D. Parker. *Chem.Commun*., 2012, **48**, 8520–852.

Synthesis, full characterization and in vitro studies of five water-soluble cyclen-based europium complexes with various numbers of the same antenna.